Andrews, S., & Berthoud, L. (2018). Modelling and Characterisation of Plasmadynamic Drag on Gridded Ion Engine Propelled Spacecraft in Very Low Earth Orbit. In *69th International Astronautical Congress, IAC 2018: Proceedings of IAC 2018, 1-5 October 2018, Bremen, Germany* International Astronautical Federation, IAF.

IAC-18-E2.2.10.x48637

Modelling and Characterisation of Plasmadynamic Drag on Gridded Ion Engine Propelled Spacecraft in Very Low Earth Orbit

Shaun Andrews[a]*, Lucy Berthoud[a#]

[a] *Department of Aerospace Engineering, University of Bristol, University Walk, Bristol, BS8 1TR, United Kingdom*
* Corresponding Author sa15339@my.bristol.ac.uk
# Supervising Academic lucy.berthoud@bristol.ac.uk

Abstract

This work presents particle-based kinetic simulations of Gridded Ion Engine (GIE) plasma plumes, in an analysis of the modified spacecraft drag profile, resultant of plume interactions with ambient thermosphere, in Very Low Earth Orbit (VLEO). VLEO is a highly appealing region for spacecraft operations, as reducing the operational height of remote sensing payloads improves radiometric performance, whilst reducing size, mass, power, and costs required of the unit. VLEO operation therefore offers high-performing economical spacecraft platforms, but the mission lifetime is very limited owing to high drag from the residual atmosphere. Detailed characterisation of plume dynamics is vital in exploring the feasibility of Electric Propulsion (EP) as a means of continuous drag compensation at such altitudes and mitigating thruster-self-induced drag mechanisms. This research considers the previously undocumented interactions between EP plumes and onset plasma flow, while also extending on the detailed studies of in-orbit drag by including interactions of EP operation.

Investigations are conducted for orbital altitudes of 150-400km, where the highest concentration of ionosphere free electrons and ions was assumed to cause most critical influence on the flow regime, modelling a prograde firing T5(UK-10) GIE. The plume expands into a rarefied environment of both neutral and charged particles, which required implementation of the hybrid 'Direct Simulation Monte-Carlo' - 'Electrostatic Particle-in-Cell' (DSMC-ESPIC) method, with density and species compositions obtained from the International Reference Ionosphere IRA-2012 and NRLMSISE-00 Atmospheric Model.

It is shown that the flow profile is affected by a combination of collisional and indirect electrostatic field mechanisms. In the immediate aft region of the spacecraft, the interaction is driven by pick-up of freestream ions within the charge-exchange cloud. The main effect of the plume is to simply deflect the thermosphere freestream as freestream ions collide with primary beam propellent and accelerate under the thruster potential. Unbounded ion jets form from collisional exchange at the primary beam edge, and where the energy of freestream ions was enough to penetrate the main plume, it was found that the plume ions may couple with the freestream to form collective electrostatic instabilities. The plume and freestream mix into an isotropic structure, which raises the possibility that far-field interactions beyond the scale investigated here may occur. The consequences of the observed plasmadynamic mechanisms on the spacecraft drag profile are theorised, and it is shown that effects of EP plume plasma in VLEO should be included in future analyses, to ensure drag models are complete.

Keywords: Electric Propulsion, Plasmadynamics, Direct Simulation Monte-Carlo, Electrostatic Particle-in-Cell, Very Low Earth Orbit, Drag.

Nomenclature

A	Thermosphere Neutral/Ion	q	Charge Density [C/m^3]
B	Magnetic Field Strength [T]	R	Thruster Radius [mm]
c	Relative Collision Speed [m/s]	t	Simulation Time [s]
d	Collision Diameter [m]	T	Absolute Temperature [K]
E	Electric Field Strength [V/m]	Γ	Gamma Flux function
h	Orbital Height [km]	u	Horizontal Velocity [m/s]
k	Boltzmann Constant [m^{2}kg/s^{2}K]	v	Vertical Velocity [m/s]
m	Particle Mass [kg]	V_e	Thruster Exhaust Velocity [km/s]
$\dot{m}$	Thruster Mass Flow Rate [mg/s]	x	Spanwise Particle Position [m]
n or nd	Number Density [#/m^3]	y	Transverse Particle Position [m]
η_{ion}	Thruster Ionisation Efficiency [%]	ω	DSMC Viscosity Index
p	Total Pressure [Pa]	ω_{pc}	Plasma Frequency [rad/s]
Pr	Generic Propellent Neutral/Ion	ϕ	Plasma Potential [V]

Subscript

0	Thruster Reference
∞	Freestream Reference
e	Electron Property
$exit$	Thruster Exit Grid
$fast$	Fast-Moving Neutral/Ion
i	Simulation Iteration
r	Particle Collision Relative Property
ref	DSMC Reference Property
S/C	Spacecraft
$slow$	Slow-Moving Neutral/Ion

Acronyms/Abbreviations

AMU	Atomic Mass Unit
CEX	Charge Exchange
DSMC	Direct Simulation Monte-Carlo
EP	Electric Propulsion
ESA	European Space Agency
ESPIC	Electrostatic Particle-in-Cell
GIE	Gridded Ion Engine
GOCE	Gravity Field and Steady-State Ocean Explorer
IRI-2012	2012 International Reference Ionosphere
LEO	Low Earth Orbit
MCC	Monte Carlo Collision
NRLMSISE-00	International Standard Atmosphere
NTC	No Time Counter
SFU	Solar Flux Unit
TSS1	Tethered Satellite System
VHS	Variable Hard Sphere
VLEO	Very Low Earth Orbit

1. Introduction

Very Low Earth Orbit (VLEO) describes the region of orbit altitudes below 400km, characterised by high rates of orbital decay from atmospheric drag. Despite this, the region remains highly appealing for spacecraft operations, providing substantial improvements in the performance of Earth observing payloads [1].

With decreasing orbit height, the spatial resolution of optical instruments increases for a constant aperture. Thus, resolution can be increased for the same payload volume or the payload volume and mass reduced for equal resolution by operating in a lower orbit. For radar payloads, reducing the operational altitude can reduce the transmitted power requirements and minimum antenna area whilst maintaining a given resolution. Furthermore, as the distance to the imaging target is reduced, the radiometric performance is improved according to the well-known inverse-square law [2]. This is significant for optical, radar, and communications-based detectors, such that the sensitivity of a given instrument can be compromised upon whilst achieving similar radiometric results. This then leads to reduced instrument cost, size, and mass.

Communications also benefit from reduced power requirements and downlink data rates. Operating the spacecraft at a lower orbit also increases the available payload mass fraction of the launch vehicle. VLEO operation therefore offers high-performing economical spacecraft platforms, but the mission lifetime is very limited owing to high drag from the atmosphere…

To maintain altitude in VLEO, a spacecraft therefore requires regular prograde manoeuvres, or a method of continuous low thrust drag compensation. The high specific impulses provided by electric propulsion (EP) systems makes the operation of such systems feasible as a means of drag compensation in VLEO. EP thrusters can allow continuous compensation for the variable deaccelerations experienced by a spacecraft due to atmospheric drag, without the vibrations and limited mission lifetime with the use of conventual chemically powered rocket engines, which are capable only of restoring the path of the host spacecraft to a purely inertial trajectory. The use of EP as a means of drag compensation was demonstrated by the European Space Agency's (ESA) Gravity Field and Steady-State Ocean Circulation Explorer (GOCE), launched in 2009. GOCE utilised dual-gridded electrostatic ion thrusters to compensate for the orbital decay losses [3], sustaining an orbital altitude of 255km for 55 months before expending its fuel.

The mission lifetime of a VLEO-dwelling spacecraft is limited by the quantity of propellent carried. The propellent required is proportional to the thrust and by extension the drag that the craft experiences. Effects introduced by the operation of a Gridded Ion Engine (GIE) have long raised several concerns. This includes plume backflow contamination and spacecraft interactions with the plume-induced plasma environment. Backflow contamination can lead to material deposition that can affect thermal control surfaces, optical sensors, photovoltaics, science instrumentation, and communications. The induced plasma environment will modify spacecraft charging characteristics and can lead to subsequent charge interactions with the ambient environment. The GIE plume will modify the properties of the VLEO thermosphere flowing around the spacecraft; directly from ambient-plume interaction, as well as indirectly via its effect on spacecraft charge and the near-spacecraft plasma environment. As a GIE will be operating continuously in a drag-compensating role, a detailed characterisation of the plume dynamics in the rarefied plasma environment of VLEO needs to be carefully assessed.

Due to the complexity of the problem, the difficulty of replicating space conditions in a laboratory, and the lack of prospects to flight test EP/GIE systems, particle-based simulations are the only suitible means to conduct research. In particular, Roy et. al. [4] conducted hybrid

particle-fluid simulations to study the effluent effects of the plume region, with detailed study on the interactions of charge-exchange backflowing propellent. Tajmar [5] characterised the influence of induced plasma environments on spacecraft charging, using various hybrid and full-particle based simulations with floating potential models of spacecraft surfaces. Merino et al [6] have developed full-fluid models of both near and far plume regions. They assessed hypersonic plume expansion in very high computational resolution. The fluid simulations were applied to determine the forces transmitted, by a GIE plasma plume, to a remote object [7]. Wang and Brophy [8, 9] have developed full-particle and hybrid models of single and multiple thruster plumes, extending their studies to the effects of static ambient environments on plasma-plume development. There have been no studies concerning other aspects of plasma-plume interactions, such as GIE operation in the VLEO thermosphere environment and plume-thermosphere interactions. To the authors knowledge, there has never been a study into the effects of GIE operation on its host spacecraft drag profile.

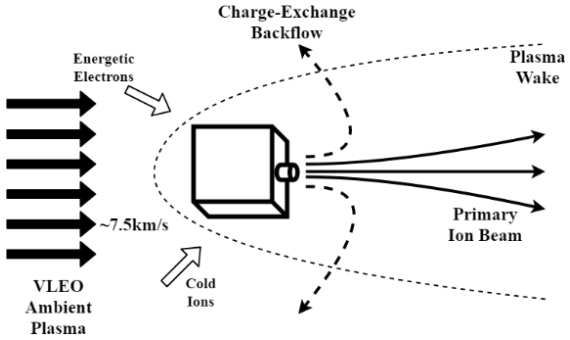

Fig. 1. The Plasmadynamic Flow Regime of GIE Propelled Spacecraft in VLEO

For a spacecraft operating in VLEO, the GIE performs in the tenuous, relatively cold plasma of the thermosphere, with a hypersonic flow speed, and within the Earth's magnetic field. A schematic overview of the regime is given in Fig. 1. It can be assumed that mechanisms by which the drag profile is modified can be categorised into three processes: 1: Particle-particle collisions between propellent neutrals/ions and freestream thermosphere neutrals/ions. 2: Accelerations to thermosphere and propellent ions due to the electrostatic field induced by GIE plasma plume, as well as the ambient plasma potential field. 3: Electrostatic accelerations to thermosphere and propellent ions because of the spacecraft surface charge potential.

While the literature describing the particle-based modelling of GIE plumes and the associated plasma interactions with spacecraft systems is extensive, most studies conducted so far have concentrated on thruster operation in vacuum environments. Wang [10, 11] has investigated the interactions between ion thruster plumes in the presence of solar wind. It was found that the solar wind was of too little density to influence the plasma environment near the thruster. But, far downstream, the plume ions coupled with those of the ambient wind plasma to result in a range of instabilities. There have been no studies concerning aspects of plume interactions in relatively denser ambient environments, such as that in VLEO.

VLEO thermosphere couplings have never been examined in association with GIE firing. The properties of an ion thruster plume expanding into the VLEO environment involves much larger number densities than those seen in solar wind plasma interactions and it is not immediately clear how significant the interactions would be in the context of spacecraft drag. There have however been thorough studies of the interactions between the Low Earth Orbit (LEO) environment and traditional chemical thruster plumes, both experimental and computational.

Bernhardt et al [12] characterised the interactions of neutral rocket plumes in static charged backgrounds, supplemented with space-based measurements in the ionosphere. Analysis by Burke et al. [13] investigated the charge-exchange backflow of the thruster firing of the Tethered Satellite System (TSS1), noting high collisional energies at the craft leading edge, induced by upstream propellent. It was found that significant scattering occurred near the thruster exit, as well as after collisions with the neutral gas and ambient oxygen ion environment, giving in detail the resulting energy distributions of freestream particles picked up by the plume [14]. The development of both the neutral plume and the freestream were found to be strongly influenced by the presence of local electromagnetic fields by Stephani and Boyd [15]. The hybrid-kinetic model that they developed demonstrated that the local environment and the magnetic field in LEO resulted in a cross-flow diffusion of the plume, increasing the density of propellant upstream and transverse far from the thruster. It is therefore a reasonable hypothesis to say that the coupled intra-electrostatic and collisional interactions, between the VLEO environment and an expanding plasma-plume, influences the particle collisions and electrostatic stress seen at spacecraft surfaces, and by extension the drag force.

Drag calculations were previously performed on satellite bodies in VLEO, to assess EP drag-compensating feasibility, by Walsh and Berthoud [16, 17]. The study modelled the VLEO environment as solely neutral, modelling ionic species as their respective uncharged particles, using the Direct Simulation Monte-Carlo (DSMC) method, and the GIE was not modelled. This research expands that study by fully modelling the GIE plume within the ambient flow, with consideration

for the charged species of the ionosphere, to capture the drag profile resulting from electrostatic mechanisms.

In this paper initial plasmadynamic drag analysis via particle-based simulations of the interaction of GIE plumes with the rarefied ambient VLEO thermosphere are presented. In section 2, an overview of plasma-plume, spacecraft and thermosphere interactions is given. In section 3, the particle-kinetic methodology and simulation setup is explained. In section 4, initial simulation results are presented. The aim within is to investigate the mechanisms governing the flow regime and the theorise the consequence upon the spacecraft drag profile. This paper discusses a qualitative analysis, and quantifying the results is ongoing. Lastly, section 5 contains conclusions and initial thoughts towards future work.

2. Plasmadynamic Interaction Phenomenon

2.1. Spacecraft Plasmadynamics in the Thermosphere

In the tenuous plasma environment of the VLEO thermosphere, the relative speed of the spacecraft vastly exceeds the ion thermal speed in the plasma and, due to the greater mass of incoming ions than electrons, the thermal speed of electrons is far greater than that of ionic or neutral species [18]. As consequence, a spacecraft surface initially experiences a larger flux of electrons than neutrals and ions, acquiring a net negative charge compared to the surrounding environment. This work shall therefore focus on the discussion of negative spacecraft surface potentials. Negative potential manifested by the build-up of charge on the spacecraft surface accelerates near ions and repels electrons. A dynamic equilibrium is established between the flux of ions and electrons in the near environment. The acceleration and repulsion of ions and electrons forms a plasma sheath; a region of charge discontinuity surrounding the spacecraft where the plasma is electrostatically shielded from the spacecraft's floating potential. This can be understood as a plasmadynamic 'boundary layer'.

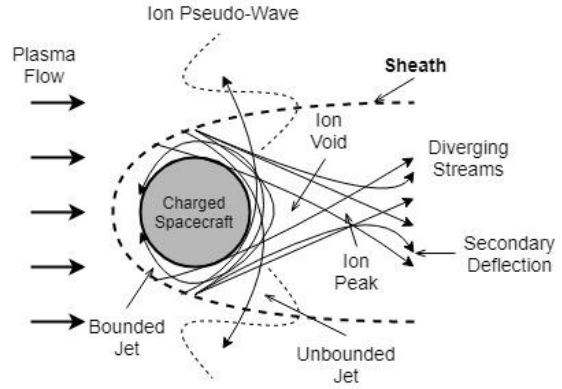

Fig. 2. Illustration of Mesothermal Flow over a Negatively Charged Spacecraft in the Thermosphere

The compression of the sheath at the leading edge, and elongation of sheath in the wake, is a result of the influence to incoming ion velocity, where hyperthermal ions are unable to penetrate the wake region aft of the spacecraft. Sub-thermal electrons however, can fill the void of the wake, creating a radial negative charge gradient trailing in the wake that will attract nearby ions and enhance the fill rate. Such conditions are described as mesothermal. The mesothermal structure of flow around a spacecraft body is summarised in the illustration of Fig. 2. The refill of the wake by deflected ions generates an ion density gradient travelling radially to the oncoming flow as ions move to fill the wake. Within the wake, the focus point of deflected ions can also generate a positive region of sufficient strength to cause a tributary deflection. This has been observed to be more prominent with spacecraft of smaller spanwise dimensions [19]. Finally, depending on where they enter the sheath, ions within certain energy groups are deflected through the near wake on unbounded (hyperbolic orbits that form ion pseudo-waves) or bounded (impact the body) trajectories [20, 21]. This anisotropic structure of plasma interactions and associated kinetic phenomena that arise from the sheath structure are difficult to assess. For such conditions, it has been common for direct and indirect plasmadynamic forces to be calculated directly from self-consistent solutions by measuring the momentum fluxes through a control surface bounding the spacecraft [22]. A recent numerical study by Capon et al [23] provides a thorough characterisation of the direct and indirect charged plasmadynamic drag mechanisms in the ionosphere.

2.2. The Gridded Ion Engine Plume

In GIEs, propellant ions are accelerated electrostatically by a system of grids to form a high velocity beam. Neutralizing electrons are emitted from a neutralising cathode. During normal GIE operation, electron emission can be assumed to keep the global plume wholly quasi-neutral and prevent the spacecraft from charging up significantly.

Although GIE systems typically possess ionisation efficiencies η_{ion}>90%, some proportion of the propellant will diffuse across the ion optics as a neutral gas. The neutral gas particles possess slow thermal velocity, remaining in high density near the thruster exit, exceeding that of the energetic ions in the primary beam. Charge-exchange (CEX) is a process which occurs when outer electron shells of a neutral atom and ion collide, resulting in electron transfer from the atom to the ion [24]. CEX collisions occur in the plume near the thruster exit, resulting in the conversion of slow-moving neutrals and fast-moving ions into fast-moving neutrals and slow-moving ions as per

$$Pr_{slow} + Pr^{+}_{fast} \rightarrow Pr_{fast} + Pr^{+}_{slow} \quad (1)$$

where Pr is representative of an arbitrary monoatomic propellant. In the absence of an electromagnetic field, the primary beam ions follow line-of-sight trajectories because the electric field within the plume is too small to perturb their motion. Hence, the primary ion beam will keep its coherent structure. The electrons are much more mobile than ions, so the centre of the plume has a positive potential. This potential causes the slowly moving CEX ions to move transversely out of the plume. The result is the formation of a CEX cloud, a torus-shaped plasma structure surrounding the primary beam near the thruster exit. The ions produced from the CEX interactions have the most detrimental impact on spacecraft operations; CEX ions scatter to regions upstream of the thruster exit. The resultant plasma sheath that forms around the spacecraft becomes highly influenced by thruster operation. The interactions of CEX ions can affect optical sensors, attenuate communication signals, cause surface erosion and charging, as well as destructive discharge [25].

3. Application of Particle-Kinetic Simulations

2.1. DSMC-ESPIC Framework

The collisions between ambient VLEO particles and ion thruster plume propellant occur under extremely low-density conditions, where traditional continuum flow methods cannot be applied. The most appropriate numerical method for simulation of the regime is the Direct Simulation Monte-Carlo (DSMC) method, originally developed by Bird [26]. It is well suited for non-equilibrium gas flow problems in which binary collisions are dominant. It models the evolution of the particle distribution function through particle collisions. The charged plasma is subject to self-consistent electrostatic fields, which requires the Electrostatic Particle-in-Cell (ESPIC) method [27]. This is a kinetic method that determines solutions to the Vlasov-Maxwell equations. In this work, the subsequent system of rarefied collisional and plasma interactions is therefore simulated in Starfish, a two-dimensional code for plasma and gas kinetics problems [28]. It implements the ESPIC method to model plasmas, with multiple gas injection sources, and a detailed surface handler for surface interactions. The species interact with each other via DSMC or Monte Carlo Collisions (MCC) or by chemical reactions.

This work uses a structured cartesian mesh which facilitates both the DSMC collisional and ESPIC electrostatic calculations. The orders of magnitude spanning the properties of electrons from ions and neutrals, makes their inclusion complex as particles within the simulation. If modelled as DSMC macroparticles, extremely small time-steps would have been required to resolve the electron behaviour, and an infeasible quantity of time required for simulations to run to steady-state. The ESPIC potential solver uses a hybrid kinetic-fluid approach to model the plasma, and it is assumed that the plasma is quasi-neutral in nature. Heavy neutral and ionic species are modelled as DSMC macroparticles, while the electrons are represented as an equilibrium fluid through momentum equations. Since this investigation concerns itself with plasmadynamic interactions in the near-field of the spacecraft, the influence of the Earth magnetic field is assumed negligible, i.e. B=0.

At each simulation time-step, first, the total number of collision pairs, within each mesh cell, is determined by a multi-species implementation of Bird's No Time Counter (NTC) method, with the collision probability determined with total collisional cross-sections per Equation 4.63 found in [26].

$$d = d_{ref}\left(\frac{[2kT_{ref}/(m_r c_r^2)]^{\omega-1/2}}{\Gamma(\frac{5}{2}-\omega)}\right)^{1/2} \tag{2}$$

Post-collision velocities are assumed to follow isotropic scattering. With DSMC collisions handled, the ESPIC approach is used to determine the acceleration on the charged particle species by the self-consistent electric field. The electron charge density is interpolated to the mesh nodes, and the local potential is then determined through the Boltzmann relationship, which approximates the plasma potential, under the quasi-neutral assumption, according to:

$$\phi = \phi_\infty + T_e \log\left(\frac{n_e}{n_\infty}\right) \tag{3}$$

The use of this relation makes several assumptions; the electron flow is treated as an isothermal, ideal gas, and the influence of intra-electromagnetic properties is neglected in the electron fluid momentum equations. The electric field is then determined as:

$$\vec{E} = -\nabla\phi \tag{4}$$

Finally, the consequent acceleration from Newtonian motion coupled with Maxwell's equations through the Lorentz force above is used to advance these macro-particles through time, using a leap-frog integration method, by imposing a velocity increment on the ions at each time step [29].

$$m_i \frac{d\vec{v}_i}{dt} = q\vec{E},\ \frac{d\vec{x}_i}{dt} = \vec{v}_i \tag{5}$$

3.2. Momentum/Charge-Exchange Collisions

The system can be considered to consist of four general sets of chemical species: propellent neutral/ions, referred to generally as Pr/Pr^+, and ambient plasma neutrals/ions A/A^+. Heavy species collisions are treated according to standard DSMC collision dynamics, with the possibility of a charge transfer for neutral/ion

collision pairs. Analysis by Rapp and Francis [30] has demonstrated that the elastic momentum exchange cross-sections and charge-exchange (CEX) cross-sections are approximately equivalent. This relationship was assumed true for this implementation, and if the collision under consideration involved a neutral-ion pair, the probability of a CEX event was taken to be 0.5, with the collisional cross-section using the data described within [31]. CEX collisions were modelled using the Monte-Carlo-Collision (MCC) method, which differs from the DSMC in that the source particles are collided with a target cloud, which does not have its properties updated. The density of the target neutrals were many orders of magnitude greater within the system of interest than the density of the source ion species. Therefore, it was considered reasonable to assume that the neutrals were affected by collisions to such a small extent as to be negligible, and the MCC method valid. The MCC method is much easier to implement and computationally less demanding, thus the simulation time was greatly reduced with this assumption. The full set of permitted interactions are shown in Table 1.

Table 1: Permitted Collision Interactions

	A	A^+	Pr	Pr^+
A	DSMC	DSMC/MCC	DSMC	DSMC/MCC
A^+	-	DSMC	DSMC/MCC	DSMC
Pr	-	-	DSMC	DSMC/MCC
Pr^+	-	-	-	DSMC

Due to the lack of data available for the representative gas properties of the species in this system at the energy levels of interest, the momentum-exchange collisions are modelled using the Variable Hard Sphere (VHS) method suggested by Bird [26, 32] with isotropic scattering of post-collisional velocities. The reference molecular diameters, reference temperatures and viscosity indices, required for representation of the species in the DSMC method, were acquired from Appendix A of [32].

3.3. Numerical Setup

The plume flow examined in this initial study models the T5 (UK-10) GIE. The T5 was chosen because of the large repository of experimental data available from vacuum chamber testing [3, 33, 34], but primarily as it was the EP system used on the GOCE spacecraft, and therefore allows simulations to be more easily compared to GOCE accelerometer data in potential future work. Under typical operating conditions, using a fuel of Xenon, the R=50mm radius thruster has a mass flow rate of $\dot{m}$ =0.677mg/s and exit beam velocity of around V_e=40km/s [35]. Near the thruster exit, the temperature of the beam ions is assumed to be that of the accelerating exit grid of T_{exit} =1000K, and the temperature of the neutralising electron fluid to be on the order of T_0=1eV. The focus of this paper considers a spacecraft with a uniform, fixed surface potential of $\phi_{S/C}$ =-10V with respect to the environment. The influence of self-consistent charging is the subject of future work.

Ionisation within the GIE chamber can produce multiple ionised propellent states. The fraction of doubly-charged ions is typically less than 10% for GIEs, and thus it was assumed the effect of these higher charge ions was negligible, and they were neglected in initial simulations. The thruster exit boundary was defined as a Maxwellian source; ions generated at a specified mass flow rate and exhaust velocity, given by the thruster operating parameters, and then a random thermal velocity is added, sampled from the Maxwellian according to the prescribed temperature of the thruster exit grid. The unionised neutrals are modelled and tracked as particles, with CEX ions generated directly from collisions between ions and neutrals. The neutrals, like the primary beam ions, are sampled with a Maxwellian distribution, with a mass flow rate determined from the thruster ionisation efficiency and null non-thermal velocity (i.e. they drift across the exit with only thermal speed).

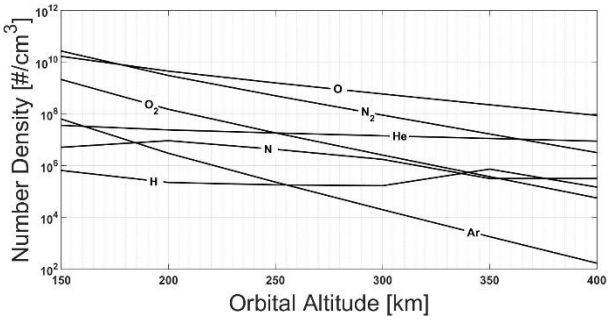

Fig. 3. Neutral Species Number Density Variation with orbital Altitude in VLEO

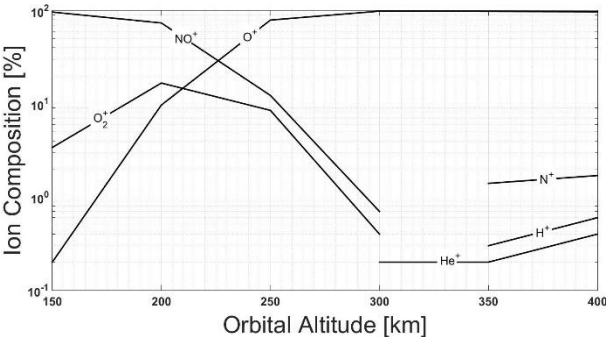

Fig. 4. Charged Species Composition Variation with orbital Altitude in VLEO

VLEO conditions were modelled using data from the International Reference Ionosphere 2012 (IRI-2012) [36] and the NRLMSISE00 Atmosphere Model [37]. This model provides temperature and gas species number densities (for He, O, N_2, O_2, Ar, H and N) covering all the range from sea level up to the exosphere. It accounts for the contribution of non-thermosphere species to the

drag at high altitudes, such as O^+ and hot oxygen (energetic oxygen atoms resulting from photochemical processes in the upper atmosphere [38]) by including a component named 'anomalous oxygen'. To correctly illustrate the full electrostatic interactions in detail, this study does not use the anomalous oxygen parameter, and instead models each ionic/energetic species individually from IRI-2012 data.

Fig. 3. And Fig. 4. present the composition parameters used in initial simulations, in the form of number density and proportions of species in their ionised states. Simulations were conducted for $150 \leq h \leq 450$km in increments of Δh=50km. At any given altitude, the properties of the ionosphere and thermosphere are not uniform, varying with the solar cycle as well as the Earth's ground topology and other local irregularities. Thus, over a single orbit in VLEO, the density and composition of the environment can vary significantly. For the initial simulations presented here, a 3-month average density and composition was calculated for the NRLMSISE00 default data of 01 Jan 2000 at 55° latitude 45° longitude, with F10.7 solar radio flux of 163.1sfu. This is a first implementation, falling between the last recorded maximum and minimum solar fluxes of 215sfu and 67sfu.

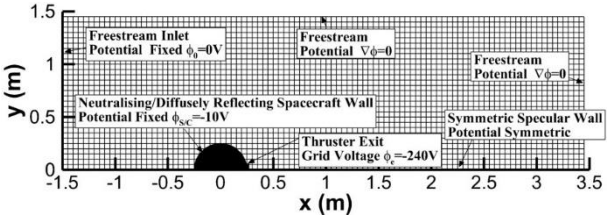

Fig. 5. Simulation Topology and Boundary Conditions. Every 5th mesh node shown for clarity.

For simulations presented within, the spacecraft is taken to be a sphere with radius 0.25m. This allows mechanisms to be preliminarily calculated within the context of the classical 'ion flow over a charged sphere'. The domain extends $-1.5 \leq x \leq 2.5$ m and $0 \leq y \leq 1.5$ m, and its topology is illustrated in Fig. 5. The spacecraft is located at $-0.25 \leq x \leq 0.25$ m and $-0.25 \leq y \leq 0.25$ m. The thruster exit grid centre is located at $x = 0.25$m, $y = 0$m, and generates thrust in the $-x$ direction, such that the plume expands in the $+x$ direction. The exit plane boundary conditions were applied according to T5 observational data from Crofton [35], and the thruster simulation parameters are shown in Table 2.

Simulations are half-domain symmetric 2D models of the spacecraft cross-section, and it is assumed the flow profile is axisymmetric in the x direction. Thermosphere flow is from left to right. The flow was taken to have velocity equal to the orbital speed at the simulated altitude. A uniform source boundary was applied at the inlet, with the mass flow rate of each species determined using the known orbital speed and number density. The freestream reference electron density n_∞ and electron temperature T_∞ were taken directly from IRI-2012. Dirichlet potential boundary conditions were applied at the freestream inlet (reference potential ϕ_∞=0), thruster exit and spacecraft surfaces. At the exit, the potential was set corresponding to the GIE accelerator grid voltage ϕ_{exit}=-240V. Neumann conditions were applied at right-hand and upper freestream boundaries.

Table 2: T5(UK-10) Simulation Parameters [35]

Parameter	Simulation Value
Radius R [mm]	50
Mass Flow Rate $\dot{m}$ [mg/s]	0.677
Exhaust Velocity V_e [km/s]	40
Exit Grid Voltage ϕ_{exit}[V]	-240
Ionisation Efficiency η_{ion}	78
Exit Temperature T_{exit}[K]	1000
Reference Potential ϕ_0[V]	0
Electron Temperature T_0[eV]	1

Gas-surface interactions are diffusely reflecting and neutralising with complete thermal accommodation to a $T_{S/C}$=500K spacecraft wall; investigation into the effect of surface temperature and surface interaction models is planned for future work. Mesh spacing was Δx=Δy=0.01m. The simulation time-step was $\delta t = 5 \times 10^{-8} s$. The time-step chosen such that it resolves ion oscillations defined by the ion plasma frequency $\delta t < \frac{\omega_p}{2}$ and ensures that simulated particles spend multiple time-steps within a single cell $\delta t < \frac{\min(\Delta x, \Delta y)}{\max(u,v)}$. The number of particles represented within each DSMC macroparticle was based on the conservative methods laid down by Boyd [39], and the simulations contained approximately 1 million particles in steady-state conditions. As the DSMC method is stochastic, a large number of particles is required to obtain meaningful statistics.

4. Results and Discussion

4.1. VLEO Thermosphere Freestream

Simulation results for the nominal case of thermosphere freestream are presented in Fig. 6. The results are given for flow at h=400km altitude, where O^+ is the dominant species. The wake formed behind the spacecraft is clearly seen. It is also clear to see the reflection of ions at the centreline, the line of symmetry. This reflection corresponds to the influx of particles from the opposite half of the simulation, and the secondary deflection of ions due to positive potential build up in the immediate wake. This is best seen in the plot of the vertical velocity in Fig. 6a. The focus point of wake ion deflection occurs at $x \approx 0.6$m, after which ions are

reflected into the freestream, with inlet conditions matched at $x \approx$3m. The plasma sheath is seen to possess thickness around the order of 5cm at the fore-body.

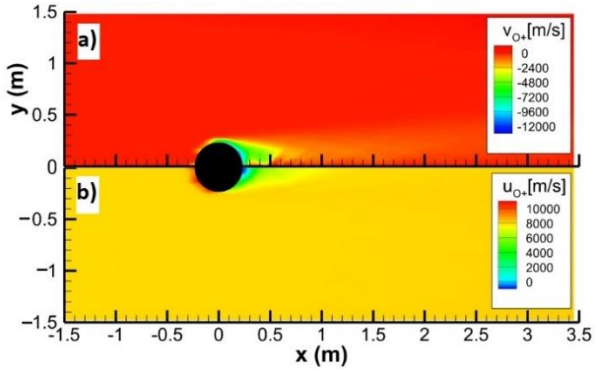

Fig. 6. a) O^+ Ion Vertical Velocity b) O^+ Ion Horizontal Velocity, h=400km Thermosphere Freestream

4.2. Vacuum GIE Firing

Fig. 7. shows the contours of plasma potential and the total Xe^+ ion density for the nominal case of the T5 GIE steady-state firing in a vacuum. The outflow of the CEX ions form the expected charge-exchange cloud, and the primary beam has a 14° divergence half angle, agreeing with the data of Crofton [35]. Once outside the plume, the CEX ions come under the influence spacecraft sheath. Outside the region of the primary beam, the CEX ions begin expansion, drawn upstream by the negative surface potential of the spacecraft. The result is an anisotropic scattering in the near exit region to the upstream near the spacecraft. The resulting expansion fan becomes a preliminary sheath of plasma downstream of the spacecraft, which turns the trajectories of the CEX ions into the upstream direction, until they enter the sheath of the spacecraft.

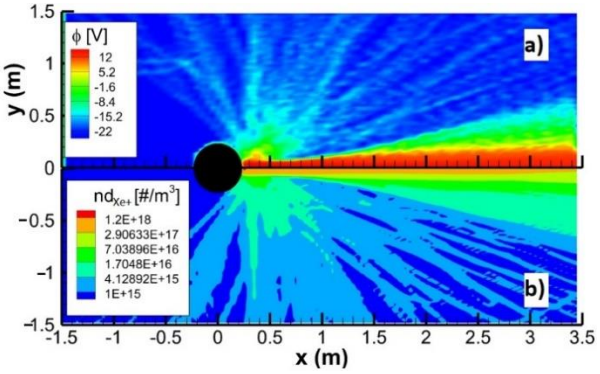

Fig. 7. a) Plasma Potential (ϕ) b) Xe^+ Number Density (nd_{Xe^+}), Vacuum Case GIE Firing

4.3. GIE Firing in VLEO Freestream

Results in this section are presented for the extreme thermosphere cases simulated: h=150km altitude where the charged environment is dominated by 95% NO^+, and h=400km where the composition is 96% O^+. The flow behaviour can thus be more clearly analysed with respect to the single foremost charged species.

The development of the freestream in terms of the ion number density is illustrated in Fig. 8. Thermosphere ions are unable to penetrate the CEX cloud of the thruster, and the ions are partially "picked up" by the plume. A high-density concentration of ions forms at the root of the CEX cloud, and collisions between thermosphere species and propellent within the CEX structure prevents refill of the wake. Momentum and CEX collisions between the relatively fast moving propellent ions and slow moving ambient, greatly reduces the velocity of the ambient ions, and they become caught in the radial electrostatic field that governs the CEX cloud, acting to reinforce the CEX structure. The result is that the distribution of the freestream tends away from the initial uniform and toward the anisotropic Maxwellian of the plume.

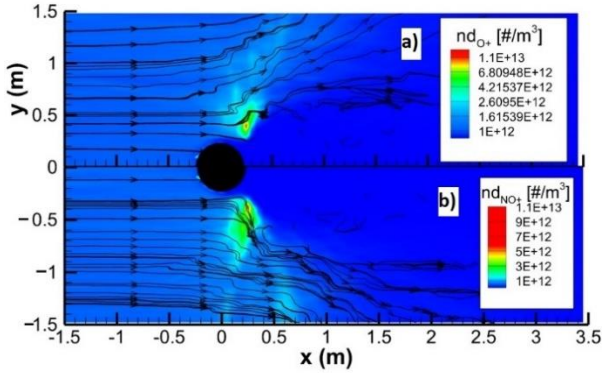

Fig. 8. Thermosphere Ion Number Density with Velocity Streamlines a) O^+ h=400km (nd_{O^+}), b) NO^+ h=150km (nd_{NO^+})

The freestream couples into a relatively warmer plasma that expands with the primary beam. The vertical velocity distribution of the thermosphere ions is shown in Fig. 9., and it indicates a definitive boundary between ions that have penetrated the primary plume, and those deflected transversely via collisions at the beam edge. At h=400km, the comparatively light O^+ ions (16amu) are accelerated to radial velocities on the order of v_{O+}=5km/s, and this velocity component is not observed to return to near freestream conditions within the domain of the simulations. The NO^+ ions (30amu), at h=150km, are seen to reach radial velocities of 2-4km/s, and the rate of deceleration toward freestream uniformity is far greater than that of the O^+, with near-zero vertical velocity returned at approximately x=3m. It is apparent that with decrease in the charged species weight (and by extension increase in orbital altitude), the freestream is more sensitive to plume deflection. It is clear that lighter species are subject to greater accelerations from kinetic

collisions at the boundary and the repelling intra-electrostatic field contained within the plume.

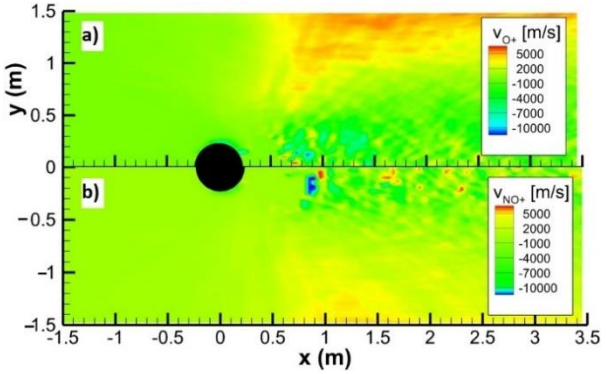

Fig. 9. Thermosphere Vertical Velocity a) O^+ h=400km (v_{O^+}), b) NO^+ h=150km (v_{NO^+})

Far downstream from the thruster exit, where the plume density has decreased to a level that the VLEO plasma can more easily penetrate the plume, it is possible the plume ions may couple with the ambient plasma through collective electrostatic effects. Fig. 9. illustrates a turbulent behaviour in the wake at x>1m, that can also be seen to contain an oscillatory pattern in the spanwise dimension. Low energy CEX ions and the energetic primary beam ions can constitute a free energy source, which may drive one of several electromagnetic instabilities into the propagation of the freestream. The instabilities can generate enhanced electrostatic field fluctuations, leading to significant particle scattering. This raises the possibility that far-field interactions may affect the plasma environment near the spacecraft, beyond the scale of the simulations here.

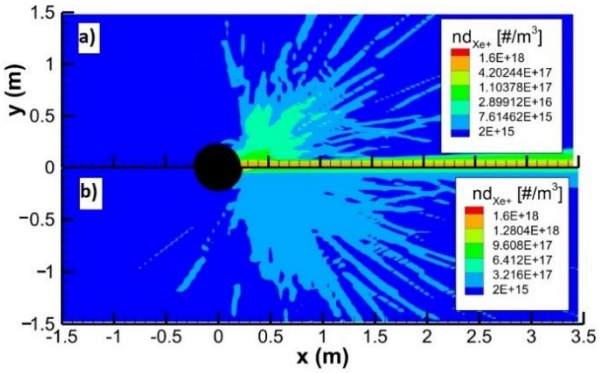

Fig. 10. Thruster Xe^+ Ion Number Density (nd_{Xe^+}), a) h=400km, b) h=150km

Fig. 10. shows the propellent ion number density distribution. The typical expansion of the CEX cloud to the upstream does not occur as is shown in Fig. 6b. The self-consistent electrostatic field contained within the tenuous ambient flow acts to damp out the large plasma potential gradient typically seen between the negative spacecraft body and the positive structure of the plume, not unlike the viscosity in continuum flows. The effect is far slower propagation of the CEX plume compared to the vacuum case, and the trajectory of CEX propellent ions appear limited to 95° with respect to the x-axis at h=400km, and narrower 82° at h=150km. The high density, heavier flow at lower altitude restricts the upstream penetration of propellent ions through the collection of positive freestream ions caught in the CEX structure; a higher concentration at lower altitude is immediately apparent in the freestream ion density comparison in Fig. 8.

4.4. Observed Interactions in the Context of Drag

The nature of the drag in these observations can be categorised into two forms. First, the direct drag, resulting from mechanical momentum exchange between particles and the spacecraft body. Second, indirect drag, manifesting itself as electrostatic field stress on the spacecraft surface, related to the Maxwell stress in the plasma flow. This results in plasmadynamic shear stress that imparts a force on the spacecraft to reflect the deformation of fields by the plasma sheath.

The introduction of an ion thruster into the regime results in a very large spanwise potential gradient across the distance of the host spacecraft, from the highly positive potential contained within the primary ion beam, with direction following the structure of the CEX cloud, culminating in the negatively charged spacecraft surface. The consequence is an electrostatic plasmasphere, that acts to deflect the freestream. Negative potential held by the spacecraft surface accelerates near ions and repels electrons, and the plasma sheath is typically compressed at the leading edge, but at approximately three-quarters span, couples to the potential field of the plume. The sheath is therefore effectively elongated to infinity in the wake and only ions with the very highest of energies can penetrate the wake region aft of the spacecraft. Electron in-fill is significantly enhanced. The ions are picked up by the plume structure and reflected around the plume boundaries, ending in trajectories parallel to the primary beam expansion.

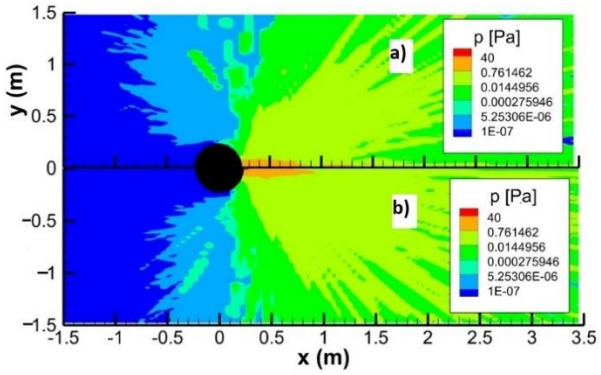

Fig. 11. Total Pressure (p) a) h=400km, b) h=150km

The process is no longer mesothermal, and the aft-spacecraft sheath thickness is that of the thruster-plume, where the momentum collisions at the primary beam edge represent a potential energy barrier. This potential barrier no longer allows ion concentration points in the flow-field where, instead of undergoing small angle deflections into the wake, ions are deflected into trajectories around the spacecraft body. This leads to formation of un-bounded ion jets external to the plume and ion pseudo-waves at the plume edge and extending within. The ion jets are clear in Fig. 8, presented as ion distributions with large radial velocities external to the plume. The influence of such reflected ion jets may manifest itself as a direct wake thrust due to momentum collisions at the freestream-plume interface. The net effect can be observed in Fig. 11. where at h=150km, the higher proportion of ions deflected with the plume increases and so too does the magnitude of the spanwise pressure gradient. This is perhaps counter-intuitive, as at lower altitudes a reduction in drag from increased wake thrust is seen despite higher flow density. This suggests that the drag on GIE propelled craft is dominated by charged species aerodynamics and not the total composition. However, the deflection of these ions must impart an indirect drag countering this direct wake thrust force. Ions that can penetrate the plume and thus into the wake also contribute to the indirect wake drag. The potential structure of the plume hides indirect effects in this qualitative assessment.

The forebody drag in this shielded flow is dominated by direct drag from sheath ion collection. Due to the electric field induced by the thruster, less compression occurs and the sheath thickness increases, and direct charged drag forces may be tend to the mechanical momentum imparted to the fore-body by an equivalently neutral flow. Indirect forebody thrust is likely to be caused by accelerated non-colliding ions with such large sheath thickness.

5. Summary and Conclusions

A DSMC-ESPIC framework for analysis of plasmadynamic ion thruster plume interactions around VLEO dwelling spacecraft, in the context of spacecraft drag, has been established.

It has been shown that the flow profile is affected by a combination of collisional and indirect electrostatic mechanisms. In the immediate aft region of the spacecraft, the interaction is driven by the pick-up of freestream ions responding to the radial electrostatic potential and high propellant concentration within the charge-exchange cloud. The main effect of the plume is to simply deflect the thermosphere freestream as freestream ions collide with primary beam propellent and come under the electrostatic acceleration of the beam expansion. This manifests as two principal mechanisms. The formation of ion jets from the collisional exchange at the primary beam edge, deflecting freestream ions on unbounded paths and, where the energy of freestream ions was enough to penetrate the main plume, it was found that the plume ions may couple with the freestream through collective plasma effects as cyclic electrostatic instabilities bounded by an ion pseudo-wave, and causing turbulence in the plume. The plume and the freestream couple into an isotropic structure which raises the possibility that far-field interactions beyond the scale investigated here may affect the plasma environment near the spacecraft.

The spacecraft drag has been theorised to exist from the collisional exchange at the plume-freestream interaction, electrostatic stress from the increased transverse ion scattering in the wake, indirect electrostatic drag from the mixing of plume and ambient ions that have penetrated the primary beam, direct momentum exchange with freestream ions impacting the forebody, and finally indirect thrust from the acceleration of non-impacting ions around the spacecraft surface by the plasma sheath.

The qualitative analysis presented in this paper only addresses the possibility and the mechanisms of VLEO thermosphere interactions with GIE plumes in the context of drag but does not attempt to quantify the effects of the individual hypothesised mechanisms or net effect on the spacecraft drag profile. Only a fixed negative spacecraft potential was considered, and the quasi-neutral model does not fully address the effects of plasmadynamic instabilities and nonequilibrium effects, including the exact behaviour of the VLEO and thruster-neutralising electrons. This will be addressed in future work, which aims to extend this study to fully-kinetic simulations, and characterise the spacecraft drag profile quantitatively, through plasma momentum balance, whilst including a self-consistent charging model of the spacecraft surfaces. Further, while the gas-surface interaction considered in this work was that of a diffusely reflecting wall with complete thermal accommodation, the exact nature of ion-surface interactions in VLEO remains uncertain in literature [40, 41]. Many sources discuss secondary electron emission, photoelectric emission and sputtering phenomena may influence both the momentum exchange between ions and the spacecraft body, changing the observed direct drag and the sheath structure, changing indirect drag forces [42]. Investigating the drag dependence on these effects, among further factors such as space weather and spacecraft geometry, will build on the frame-work presented here, all of which represent important steps toward characterising the interactions between GIE plumes in the VLEO environment. Understanding of the plasmadynamics is vital to the design and implementation of GIE propelled craft, as well as the feasibility of any VLEO mission, especially with

concepts such as air-breathing propulsion coming of age. This study has shown that effects of GIE plume plasma in VLEO should be included in future analyses, to ensure drag models are complete. These interactions will highly constrain EP implementation on spacecraft, thus must be assessed to design and select EP architectures. This study also hints that, with the deflective nature of the propellent plasma on the ambient flow, plasmadynamic flow control with EP systems is possible, and would be a very achievable means of drag reduction in VLEO.

Acknowledgements

The author would like to express thanks to Prof. Lucy Berthoud, University of Bristol, for her guidance, encouragement and useful evaluations in supervision of this work. Thanks are also given to Mr. Jonathan Walsh, PhD student, University if Bristol, for the very useful discussions concerning his work and DSMC simulations. Further appreciations are given to Dr. Lubos Brieda, Particle in Cell Consulting LLC, for his assistance and advice concerning the development of the Starfish programme.

This paper represents the UK undergraduate entry in the 46th student conference competition on behalf of the British Interplanetary Society.

References

[1] D. G. Fearn, "Economical Remote Sensing from a Low Altitude," *Acta Astronautica,* vol. 56, no. 5, pp. 555-572, 2005.

[2] J. V. Llop, P. . Roberts, Z. . Hao, L. R. Tomas and V. . Beauplet, "Very Low Earth Orbit mission concepts for Earth Observation: Benefits and challenges.," , 2014. [Online]. Available: https://escholar.manchester.ac.uk/uk-ac-man-scw:286351. [Accessed 16 9 2018].

[3] N. Wallace, P. Jameson, C. Saunders, M. Fehringer and C. Edwards, "The GOCE Ion Propulsion Assembly Lessons Learnt from the First 22 Months of Flight Operations," in *International Electric Propulsion Conference, IEPC-2011-327*, Wiesbaden, 2011.

[4] R. I. S. Roy, D. E. Hastings and N. A. Gastonis, "Ion-thruster plume modeling for backflow contamination," *Journal of Spacecraft and Rockets,* vol. 33, no. 4, pp. 525-534, 1996.

[5] M. . Tajmar, M. . Tajmar, J. . Gonz-Uuml, . . lez and A. . Hilgers, "Modeling of Spacecraft-Environment Interactions on SMART-1," *Journal of Spacecraft and Rockets,* vol. 38, no. 3, pp. 393-399, 2001.

[6] M. . Merino, F. . Cichocki and E. . Ahedo, "A collisionless plasma thruster plume expansion model," *Plasma Sources Science and Technology,* vol. 24, no. 3, p. 035006, 2015.

[7] F. . Cichocki, M. . Merino, E. . Ahedo, M. . Smirnova, A. . Mingo and M. . Dobkevicius, "Electric Propulsion Subsystem Optimization for “Ion Beam Shepherd” Missions," *Journal of Propulsion and Power,* vol. 33, no. 2, pp. 370-378, 2017.

[8] J. . Wang, J. . Brophy and D. . Brinza, "3-D Simulations of NSTAR Ion Thruster Plasma Environment," , 1996. [Online]. Available: https://trs.jpl.nasa.gov/handle/2014/26028. [Accessed 16 9 2018].

[9] J. . Wang and J. . Brophy, "3-D Monte-Carlo particle-in-cell simulations of ion thruster plasma interactions," , 1995. [Online]. Available: https://trs.jpl.nasa.gov/handle/2014/30718. [Accessed 16 9 2018].

[10] J. Wang, "Ion Thruster Plume Plasma Interactions in the Solar Wind," 1997. [Online]. Available: http://erps.spacegrant.org/uploads/images. [Accessed 16 9 2018].

[11] J. Wang, J. Brophy and D. Brinza, "A Global Analysis of Ion Thruster Plume Interactions for Interplanetary Spacecraft," 1997. [Online]. Available: http://arc.aiaa.org/doi/pdf/10.2514. [Accessed 16 9 2018].

[12] P. A. Bernhardt, J. O. Ballenthin, J. L. Baumgardner et. al., "Ground and Space-Based Measurement of Rocket Engine Burns in the Ionosphere," *IEEE Transactions on Plasma Science,* vol. 40, no. 5, pp. 1267-1286, 2012.

[13] J. S. Machuzak, W. J. Burke, L. C. Gentile, V. A. Davis, D. A. Hardy and C. Y. Huang, "Thruster effects on the shuttle potential during TSS 1," *Journal of Geophysical Research,* vol. 101, no. , pp. 13437-13444, 1996.

[14] W. J. Burke, L. C. Gentile, J. S. Machuzak, D. A. Hardy and D. E. Hunton, "Energy distributions of thruster pickup ions detected by the Shuttle Potential and Return Electron Experiment during TSS 1," *Journal of Geophysical Research,* vol. 100, no. , pp. 19773-19790, 1995.

[15] K. A. Stephani and I. D. Boyd, "Detailed modeling and analysis of spacecraft plume/ionosphere interactions in low earth orbit," , 2013. [Online]. Available: https://experts.illinois.edu/en/publications/detailed-modeling-and-analysis-of-spacecraft-plumeionosphere-inte. [Accessed 16 9 2018].

[16] J. A. Walsh and L. . Berthoud, "Is it possible to integrate Electric Propulsion thrusters on Very-

Low Earth Orbit Microsatellites?," , 2016. [Online]. Available: http://research-information.bristol.ac.uk/files/78838133/3125242_walsh.pdf. [Accessed 16 9 2018].

[17] J. A. Walsh and L. Berthoud, "Reducing Spacecraft Drag in Very Low Earth Orbit Through Shape Optimisation," in *European Conference for Aeronautics and Aerospace Sciences, EUCASS2017-449*, Milan, 2017.

[18] D. . Hastings, H. . Garrett and . . yes, Spacecraft-Environment Interactions, ed., vol. , , : Cambridge University Press, , p. .

[19] N. H. Stone, "The aerodynamics of bodies in a rarefied ionized gas with applications to spacecraft environmental dynamics," , 1981. [Online]. Available: https://ntrs.nasa.gov/search.jsp?r=19820007243. [Accessed 16 9 2018].

[20] A. R. Martin, "A review of spacecraft/plasma interactions and effects on space systems," *Journal of the British Interplanetary Society*, vol. 47, no. 4, pp. 134-142, 1994.

[21] J. C. Taylor, "Space Physics with Artificial Satellites . By Ya. L. Al'pert, A. V. Gurevich and L. P. Pitaevskii. Translated from Russian by H. H. Nickle. Consultants Bureau, N.Y.1965. 240 pp. $25.00.," *Journal of Plasma Physics*, vol. 1, no. 03, pp. 382-385, 1967.

[22] D. M. Prieto, B. P. Graziano and P. . Roberts, "Spacecraft drag modelling," *Progress in Aerospace Sciences*, vol. 64, no. , pp. 56-65, 2014.

[23] C. J. Capon, M. . Brown and R. R. Boyce, "Direct and indirect charged aerodynamic mechanisms in the ionosphere," *Advances in Space Research*, vol. 62, no. 5, pp. 1090-1101, 2018.

[24] D. Goebel and J. Katz, Fundamentals of Electric Propulsion: Ion and Hall Thrusters, New Jersey: Wiley, 2008.

[25] M. Curruth and E. Pawlik, "Interactions between a Spacecraft and an Ion Thruster-Produced Environment," *Electric Propulsion and Its Applications to Space Missions*, pp. 787-798, 1981.

[26] G. Bird, The DSMC Method, CreateSpace Independant Publishing Platform, 2013.

[27] A. B. Langdon and C. K. Birdsall, Plasma Physics via Computer Simulation, ed., vol. , , : McGraw-Hill, 1985, p. .

[28] L. Brieda and M. Keidar, "Development of the Starfish Plasma Simulation Code and Update on Multiscale Modeling of Hall Thrusters," in *48th AIAA Joint Propulsion Conference, AIAA-2012-4015*, Atlanta, 2012.

[29] L. Brieda, "Starfish User's Guide," 2018. [Online]. Available: https://www.particleincell.com/starfish. [Accessed 12 September 2018].

[30] D. . Rapp and W. E. Francis, "Charge Exchange between Gaseous Ions and Atoms," *Journal of Chemical Physics*, vol. 37, no. 11, pp. 2631-2645, 1962.

[31] J. S. Miller, S. . Pullins, D. J. Levandier, Y.-H. . Chiu and R. A. Dressler, "Xenon charge exchange cross sections for electrostatic thruster models," *Journal of Applied Physics*, vol. 91, no. 3, pp. 984-991, 2002.

[32] G. Bird, Molecular Gas Dynamics and the Direct Simulation of Gas Flows, Oxford: Oxford Univ. Press, 1994.

[33] J. E. Pollard, "Plume Measurments with the T5 Xenon Ion Thruster.," , 1994. [Online]. Available: http://oai.dtic.mil/oai/oai?verb=getrecord&metadataprefix=html&identifier=ada288697. [Accessed 16 9 2018].

[34] J. Pollard, "Plume angular, energy, and mass spectral measurements with the T5 ion engine," in *31st Joint Propulsion Conference and Exhibit, Joint Propulsion Conferences, AIAA-95-2920*, San Diego, 1995.

[35] M. Crofton, "Evaluation of the T5 (UK-10) Ion Thruster: Summary of Principal Results," in *IEPC-95-91*, 1995.

[36] D. . Bilitza, "International reference ionosphere (1990)," *Planetary and Space Science*, vol. 40, no. 4, p. 544, 1992.

[37] A. E. Hedin, "Extension of the MSIS thermosphere model into the middle and lower atmosphere," *Journal of Geophysical Research*, vol. 96, no. 2, pp. 1159-1172, 1991.

[38] J. M. Picone, A. E. Hedin, D. P. Drob and A. C. Aikin, "NRLMSISE-00 empirical model of the atmosphere: Statistical ...," *Journal of Geophysical Research: Space Physics*, vol. 107, no. A12, p. 1468, .

[39] I. Boyd, "Conservative Species Weighting Scheme for The Direct Simulation Monte Carlo Method," *Journal of Thermophysics and Heat Transfer*, vol. 10, no. 4, pp. 579-585, 1996.

[40] P. M. Mehta, A. C. Walker, C. A. McLaughlin and J. . Koller, "Comparing Physical Drag Coefficients Computed Using Different Gas-Surface Interaction Models," *Journal of Spacecraft and Rockets*, vol. 51, no. 3, pp. 873-883, 2014.

[41] F. A. Herrero, "The drag coefficient of cylindrical spacecraft in orbit at altitudes greater than 150 km," , 1983. [Online]. Available: https://ntrs.nasa.gov/search.jsp?r=19830021023. [Accessed 16 9 2018].

[42] G. A. Bird, "The Flow About a Moving Body in the Upper Ionosphere," *Journal of the Aerospace Sciences*, vol. , no. , p. , 2012.

[43] R. I. S. Roy, D. E. Hastings and S. . Taylor, "Three-Dimensional Plasma Particle-in-Cell Calculations of Ion Thruster Backflow Contamination," *Journal of Computational Physics*, vol. 128, no. 1, pp. 6-18, 1996.